Magneto-optical properties of the $Ga_xIn_{1-x}Se$ system near the fundamental band gap

G. Saintonge and J. L. Brebner
Département de Physique, Université de Montréal, Case Postale 6128, Succursale A, Montréal, Québec, Canada H3C 3J7
(Received 23 February 1984)

We have studied the magneto-optical properties of the $Ga_xIn_{1-x}Se$ system in the indium-rich and gallium-rich regions near the fundamental band gap by wavelength-modulation spectroscopy at 10 K with the electric vector $\vec{E}$ perpendicular to the $\vec{C}$ axis of the crystal. For the first time, Landau levels have been observed in InSe from which we obtain the reduced effective mass perpendicular to $\vec{C}$, $\mu_\perp=(0.090\pm0.010)m_0$. The $n=1$, 2, and 3 exciton lines were observed as a function of the applied magnetic field, permitting us to evaluate the dependence of the effective Rydberg constant, the diamagnetic shift $\epsilon_\perp\epsilon_\parallel$, the exciton Bohr radius $\epsilon_\parallel$, the band gap, and $\mu_\perp$ on the compositional parameter x. Finally, we give evidence for the presence of the γ and ϵ polytypes in the alloy system due to stacking faults.

I. INTRODUCTION

The magneto-optical properties of GaSe have been studied in great detail[1–3] and there has recently been some work published on InSe.[1,2] In this paper we examine the magneto-optical properties of the mixed crystal system $Ga_xIn_{1-x}Se$ near the fundamental gap for $0\leq x\leq 0.2$ and $0.75\leq x\leq 1.0$.

GaSe and InSe belong to the family of III-VI compounds that crystallize in a layer structure. These two compounds are isomorphic and the fourfold layers are made up of a stacking sequence Se-*M*-*M*-Se, where *M* is either In or Ga. The bonding within the fourfold layers is primarily covalent and strong whereas the bonding between the fourfold layers is of the van der Waals type and weak. The $Ga_xIn_{1-x}Se$ alloys are taken to have the same crystal structure as the end members, the principal difference being the random mixture of Ga and In in the *M* sites in the proportion of x and $1-x$.

The experimental results presented here were obtained by wavelength-modulation spectroscopy of samples at 10 K placed in a magnetic field of up to 4.8 T. The spectral region studied was in the neighborhood of the fundamental gap. Landau levels were observed in InSe allowing the determination of $\mu_\perp$, the reduced effective mass perpendicular to the $\vec{C}$ axis.[1] For GaSe, the observed Landau levels were found at the energies reported previously.[3–5] In addition, three exciton levels were found throughout the range of alloys studied with the exception of the sample with $x=0.80$. These levels were studied as a function of magnetic field and the diamagnetic shift was evaluated.

From these measurements, we have obtained the variation with composition of several parameters, namely, the energy gap, the effective Rydberg constant, the diamagnetic shift, the Bohr radius of the $n=1$ exciton line, the dielectric constant product $\epsilon_\perp\epsilon_\parallel$ as well as a second measure of $\mu_\perp$. In addition to the three exciton lines, we find evidence of a structure between the $n=1$ and 2 exciton lines in the majority of the spectra.

In the following section we describe the experimental configuration and present the results obtained. In Sec. III we give details of the interpretation of the results, and in the final section the conclusions are drawn.

II. EXPERIMENTS AND RESULTS

Crystals of $Ga_xIn_{1-x}Se$ with $0\leq x\leq 0.2$ and $0.75\leq x\leq 1$ were prepared in our laboratory by the Bridgman method. The elements were mixed in nonstoichiometric proportions: For example, InSe was prepared from a mixture of In and Se in the proportions by weight of 110 and 90. The quality of the monocrystals produced was highest for the smallest and largest values of x and tended to become poorer as x approached values corresponding to the solubility limits when several regions of differing composition were found.

Thin samples (thickness of the order of 1 to 5 μm) were cleaved from the ingots such that the $\vec{C}$ axis was perpendicular to their surfaces. (The surface area was of the order of several mm^2.) In order to minimize strain effects, the samples were glued at one corner to a copper sample holder which was then installed in an Oxford cryostat containing a superconducting magnet capable of producing a field up to 4.8 T. The temperature of the samples was determined by a calibrated germanium resistor mounted on the sample holder.

The samples were mounted in the Faraday geometry with the $\vec{C}$ axis parallel to the direction of propagation of the incident radiation. Consequently, for all the measurements reported here, the electric field vector of the radiation $\vec{E}$, the magnetic field of the magnet $\vec{H}$, and the $\vec{C}$ axis were oriented in the following way: $\vec{E}\perp\vec{C}\parallel\vec{H}$.

The monochrometer used was a 1-m Jarrel-Ash instrument modified by the addition of an oscillating mirror mounted in front of the exit slit, thus giving wavelength modulation. For small modulation amplitudes, this allowed the derivative of the transmission to be measured directly as a function of wavelength.[6] The transmitted light was measured by a GaAs photomultiplier (Hammamatsu model no. R636). The experiment was entirely

automated under the control of an Apple II + microcomputer together with a model HP2240A process controller from Hewlett-Packard.

Neutron activation measurements were made on the crystals to determine their real compositions. For the indium-rich alloys GaSe, InSe, and $Ga_{0.982}In_{0.018}$ the compositions were uniform and near the nominal values, whereas for the rest of the gallium-rich alloys a compositional gradient within the crystals were observed. Since the average composition of each was approximately equal to the nominal one, we chose to use these values as their real composition.

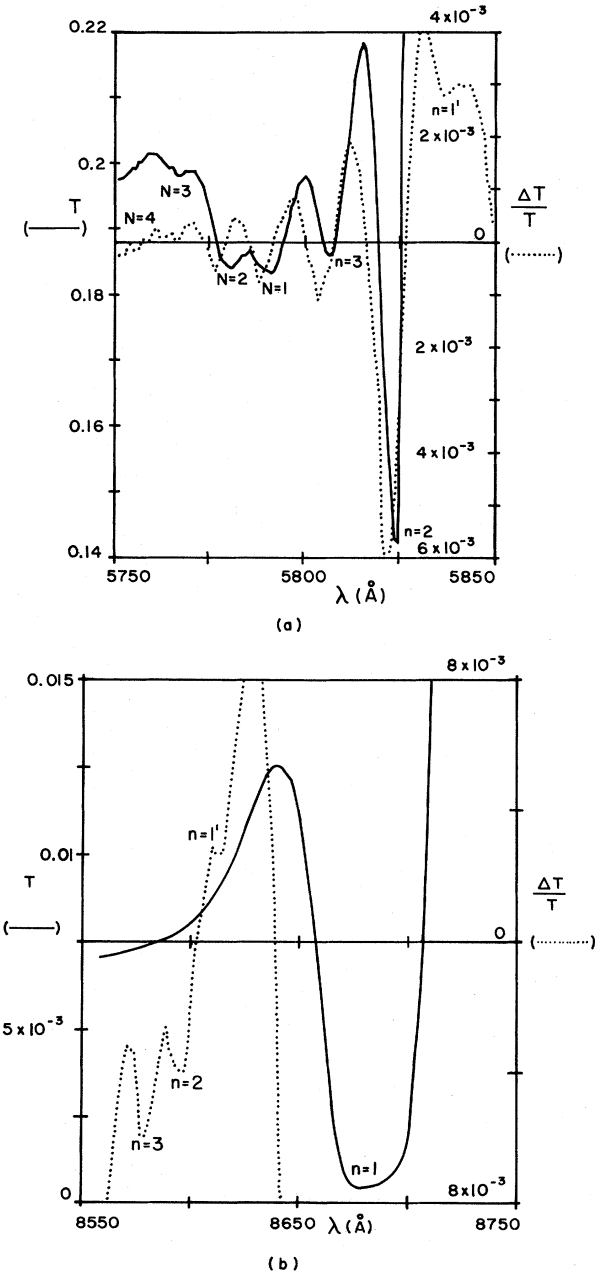

FIG. 1. Transmission (T) and modulated transmission ($\Delta T/T$) curves of (a) GaSe and of (b) $Ga_{0.162}In_{0.838}$ as a function of the energy of the incident radiation, for $H=4.7$ T and a temperature of 10 K. The solid and dotted lines are, respectively, for T and $\Delta T/T$. The structures identified by N and n are, respectively, Landau levels and exciton lines.

Typical transmission results are presented in Fig. 1, where in Fig. 1(a) the Landau levels of GaSe along with the higher order exciton lines are shown; the $n=1'$ structure is an additional line situated between the $n=1$ and 2 exciton levels. Figure 1(b) represents the transmission curves of $Ga_{0.162}In_{0.838}Se$ in the excitonic region; we can easily see the three exciton lines along with the $n=1'$ structure. On these graphs, the full lines are the transmission curves (T) and the dotted ones are the modulation curves ($\Delta T/T$); one can see the great enhancement of the structures in the $\Delta T/T$ curves compared to the transmission spectra.

Figure 2 shows a fan chart of the exciton peaks and the Landau levels as a function of the magnetic field in InSe; N is for Landau levels and n is for the excitonic lines. Apart from the $n=1$ direct exciton, structures are only visible in the wavelength-modulated spectra. Figure 3 shows the diamagnetic shift of the $n=1$ exciton in InSe as well as a change in the form of the peak which will be discussed later.

The experiments allowed the observation of three excitonic lines for all the crystals except the $Ga_{0.80}In_{0.20}Se$ one; diamagnetic shifts have been seen for $x=0.000$, $x=0.101$, $x=0.75$, $x=0.85$, $x=0.982$, and $x=1.000$; the $n=1'$ exciton was also visible for the majority of the crystals. Finally, Landau levels were resolved for GaSe and InSe.

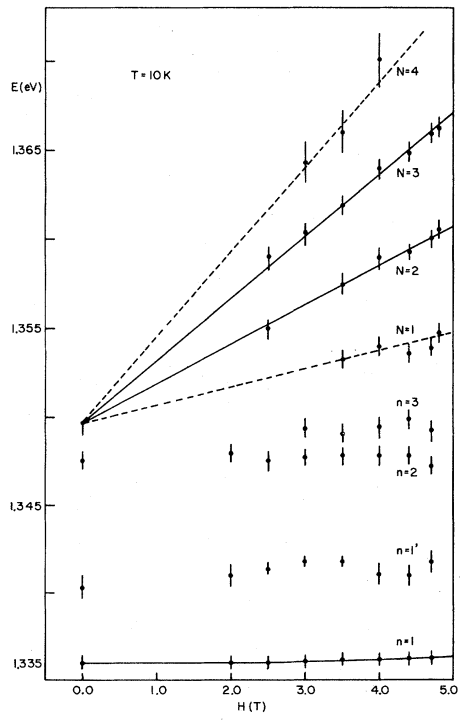

FIG. 2. Fan chart of the magneto-optical properties of InSe at 10 K. The $n=1,1',2,3$ exciton lines are presented along with the $N=1$, 2, 3, and 4 Landau levels.

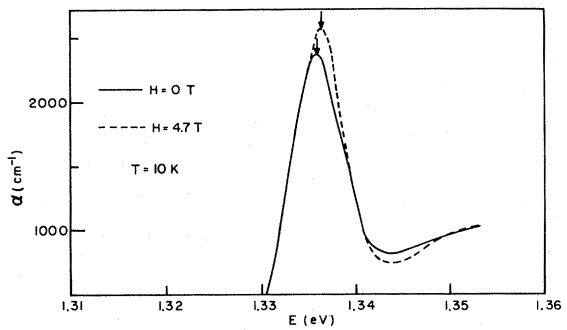

FIG. 3. Shape of the $n=1$ exciton absorption peak for $H=4.7$ T (dashed line). The arrows indicate the diamagnetic shift. The change in the shape of the two peaks is also evident.

III. DISCUSSION

A. Landau levels

The solid straight lines shown for the $N=2$ and 3 levels in Fig. 2 were evaluated by least-squares calculations whereas the (dashed) straight lines shown for the $N=1$ and 4 peaks were calculated using the same parameters as for the $N=2$ and 3 levels (changing only N), because there were not enough data points to justify a least-squares analysis. Since Landau levels follow the law

$$E=(N+\tfrac{1}{2})\hbar\omega_c,\quad \omega_c=\frac{eH}{\mu_\perp} \tag{1}$$

we obtain $\mu_\perp=(0.090\pm0.010)m_0$, where $\mu_\perp$ is the reduced effective mass perpendicular to the $\vec{C}$ axis and m_0 is the free electron mass. This value for $\mu_\perp$ is in agreement with the one deduced by Camassel *et al.*[7] but somewhat different from the value obtained by Merle *et al.*[2] From Eq. (1), we can extrapolate to $H=0$ and hence obtain a value for the band gap energy: The extrapolation gives an energy of (1.3497±0.0004) eV which is slightly smaller than the band gap as determined below from the exciton lines.

The results for the Landau levels in GaSe give a mass $\mu_\perp=(0.142\pm0.005)m_0$, which is in good agreement with the value determined by Mooser *et al.*[3] All the parameters evaluated via Landau levels analysis are presented in Table I.

B. Exciton series

The effective Rydberg constant is given for layered structures by[3]

$$R^{\rm ex}=\frac{\mu_\perp e^4}{32\pi^2\hbar^2\epsilon_0^2\epsilon_\perp\epsilon_{||}}, \tag{2}$$

where $\epsilon_\perp$ and $\epsilon_{||}$ are, respectively, the dielectric constants perpendicular and parallel to the $\vec{C}$ axis. Assuming a hydrogenlike series for the exciton, we can evaluate the Rydberg constants for all the alloys by the following relationships:

TABLE I. List of the parameters evaluated from the Landau levels and exciton lines in $Ga_xIn_{1-x}Se$ as a function of x.

x	E_1^{ex} (meV)	R^{ex} (meV)	σ_1 [10^{-5} meV/(kG)^2]	$\epsilon_\perp\epsilon_{||}$	$\epsilon_\perp$	$\epsilon_{||}$	a_1^{ex} (Å)	$\mu_\perp^{ex}$ (m_0)	$\mu_\perp^{NL}$ (m_0)	E_G^{ex} (meV)	E_G^{NL} (meV)
0.000	1336.0±0.3	15.0±0.5	14 ±2	81±8	9.60	8.4±0.8	52±4	0.089±0.013	0.090±0.010	1351.0±0.5	1350.0±0.5
0.058	1366.0±0.3	14.6±0.8			9.63					1380.6±0.5	
0.101	1392.8±0.3	15.7±0.6	8 ±2	95±9	9.66	9.8±1.0	47±5	0.11 ±0.01		1408.5±0.5	
0.162	1428.4±0.3	17.5±0.6			9.70					1445.9±0.5	
0.75	2080.3±0.3	20 ±1			10.05					2100 ±0.5	
0.80	2089.5±0.3				10.08						
0.85	2095.9±0.3	20.5±0.6	9 ±2	66±7	10.11	6.5±0.7	43±5	0.10 ±0.1		2116.5±0.5	
0.982	2106.6±0.3	20.5±0.6	5.0±0.5	90±9	10.19	8.8±0.9	37±3	0.135±0.005		2127.1±0.5	
1.000	2110.8±0.3	21.4±0.5	5.0±0.5	82±8	10.20	8.0±0.8	34±2	0.130±0.005	0.142±0.005	2132.2±0.5	2132.0±0.5

$$R^{ex}=\tfrac{4}{3}(E_2^{ex}-E_1^{ex}) ,$$
$$R^{ex}=\tfrac{9}{8}(E_3^{ex}-E_1^{ex}) . \quad (3)$$

The diamagnetic effect on the exciton is given by:[3]

$$E_n^{ex}=E_n^{ex}(0)+\sigma_n H^2 , \quad (4)$$

where H is the applied magnetic field and the subscript n refers to the exciton line. For the $n=1$ line,[4] we have

$$\sigma_1=\frac{e^2}{16\pi\epsilon_0 m_0 c^2}a_B^2\left[\frac{m_0}{\mu_\perp}\right]^3\epsilon_\perp\epsilon_{||} , \quad (5)$$

where $a_B=4\pi\epsilon_0\hbar^2/(m_0e^2)$ is the Bohr radius of the hydrogen atom. Combining Eqs. (2) and (5) results in the elimination of the product $\epsilon_\perp\epsilon_{||}$, thus giving

$$R^{ex}\sigma_1=\frac{\hbar^2e^2}{32\pi\epsilon_0c^2\mu_\perp^2} . \quad (6)$$

Hence, we can determine by a second independent relation the mass $\mu_\perp$ which then allows the determination of $\epsilon_\perp\epsilon_{||}$ and the exciton Bohr radius a_1^{ex} by the following equation:

$$a_1^{ex}=a_B\frac{m_0}{\mu_\perp}(\epsilon_\perp\epsilon_{||})^{1/2} . \quad (7)$$

Since the values of the refractive index perpendicular to the $\vec{C}$ axis are known for InSe (Ref. 8) and GaSe,[9] we can evaluate $\epsilon_\perp$ for $Ga_xIn_{1-x}Se$ by a simple linear interpolation, which should give values not too far from the real ones.

All the parameters determined by the above equations are presented in Table I along with the results of the Landau-level analysis. The σ_1 evaluations were performed by a least-squares-fit calculation.

As can be seen in Table I, the diamagnetic shifts become less and less important as one goes from InSe to GaSe. This arises from a diminution of the exciton Bohr radius and of the dielectric constant when x goes from zero to unity. We can also see that $\epsilon_{||}$ is always smaller than $\epsilon_\perp$; this is an illustration of the anisotropic character of $Ga_xIn_{1-x}Se$. The difference is small though, and it underlines the fact that even if the crystals show anisotropic behavior, they are still tridimensional structures. This fact is also illustrated by the size of the Bohr radius which indicates that the exciton extends over more than one layer.

It should be mentioned that the values for $\sigma_\perp$, $\mu_\perp$, $\epsilon_\perp$, and $\epsilon_{||}$ obtained here by the exciton results do not correlate with the values presented by Merle *et al.*,[2] as pointed out elsewhere.[1] The value obtained for $\mu_\perp$ from these results is the same as the one obtained by the Landau-level measurements, as can be seen in Table I. Furthermore, the values that we have obtained for $\epsilon_\perp$ and $\epsilon_{||}$ are such that $\epsilon_{||}<\epsilon_\perp$, which is what is supposed to happen in such a crystalline structure: this is not the case with the results of Merle *et al.*[2]

Another interesting fact is shown in Fig. 4 where the evolution of the three exciton levels is plotted as a function of the compositional parameter x. First of all, for

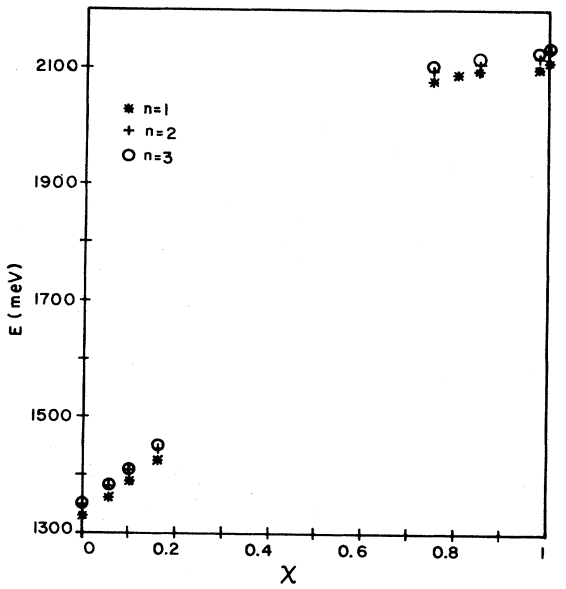

FIG. 4. Evolution of the $n=1$ (*), $n=2$ (+), $n=3$ (○) exciton lines as a function of the compositional parameter x for $H=0.0$ T and at 10 K.

the two regions (i.e., the gallium-rich and the indium-rich), the behaviors of the exciton lines with respect to x are both linear; the slopes for the $n=1$ exciton, as calculated by a least-squares approach, are

(111±10) meV; $r^2=0.99$, $x=0.75$

(574±15) meV; $r^2=1.00$, $x=0.162$.

We can easily see that, even though the qualitative behavior is the same in the two regions, they are different quantitatively. Indeed, by extrapolating each of the straight lines towards the limiting value of the other regions, i.e., $x=0$ for the gallium-rich region and $x=1$ for the indium-rich region, the predicted $n=1$ exciton levels would then be

(1905±15) meV for GaSe

and

(1999±10) meV for InSe

as compared to the real values which are

2110.8 meV for GaSe ,

1336.0 meV for InSe .

It seems as though the gallium-rich and indium-rich regions do not behave in the same way, at least as far as their electronic properties are concerned. This is surely related to the intrinsic instabilities present in this alloy system as outlined by Nishina and Kuroda.[9] The middle region, i.e., when x falls between 0.3 and 0.6 approximately, seems to act as a buffer between the gallium-rich and indium-rich domains. During the crystal growth of the alloys, different solidification processes for the two regions, which arise because of problems in the mutual solu-

bility, have probably induced differences in their behavior. It is important at this time to clarify the following point: When it is stated that the two regions behave differently as far as their electronic properties are concerned, it does not imply that there is a difference in the crystal structures of the alloys. What seems more likely is that the contributions of the three types of atoms to the exciton behavior are different for the two regions.

C. Additional exciton structures

As mentioned previously, an additional structure has been observed between the $n=1$ and 2 exciton and has been given the $n=1'$ annotation. This structure was separated from the $n=1$ exciton by energies varying from about 5 meV for InSe up to approximately 12 meV for GaSe. In GaSe the splitting of the $n=1$ exciton between the γ-ϵ mixture and the β polytype is of the order of 50 meV, whereas the separation of the $n=1$ line within the γ-ϵ mixture is of the order of 10 meV. Hence, we suggest that the $n=1'$ line is a manifestation of stacking faults in the crystal structure resulting in a coexistence of the ϵ and γ polytypes within the same crystal.

Figure 3 shows an example of another feature of the influence of the applied magnetic field on the excitonic properties. We can see a change in the $n=1$ line shape with the magnetic field. This change, apart from the diamagnetic effect which shifts the lines, becomes more pronounced with increasing magnetic field. It seems then to indicate an increase either of the oscillator strength or of the exciton lifetime.

IV. CONCLUSIONS

In the present study we have presented experimental facts related to the electronic properties of the $Ga_xIn_{1-x}Se$ alloy system by performing magneto-optical measurements. Landau levels were observed for GaSe and InSe. The results thus obtained for GaSe are similar to those presented elsewhere[3] whereas the results for InSe are new and enabled us to determine $\mu_\perp$.

Three exciton levels were observed for all the alloys except for $x=0.80$. From these measurements, parameters such as $\mu_\perp$, $\epsilon_\perp\epsilon_{||}$, $\epsilon_{||}$, E_G, R^{ex}, σ_1, and a_1^{ex} were evaluated as a function of x. The hierarchy $\epsilon_{||}<\epsilon_\perp$ is a confirmation of the anisotropic character of the alloy system but the relatively small difference between the values of these two parameters is an indication that we still have to deal with a three-dimensional structure.

The behavior of the three exciton lines with the compositional parameter x suggests that the electronic behavior in the indium-rich and gallium-rich regions is not the same even though the crystalline structure does not change.

For the majority of the alloys, an additional exciton line, labeled $n=1'$, was seen and interpreted as evidence of stacking faults in the structure resulting in a mixture of the γ and ϵ polytypes.

[1]G. Saintonge and J. L. Brebner, Solid State Commun. **44**, 1625 (1982).
[2]J. C. Merle, R. Bartiromo, E. Borsella, M. Piacentini, and A. Savoia, Solid State Commun. **28**, 251 (1978).
[3]E. Mooser and M. Schlüter, Nuovo Cimento **18B**, 164 (1973).
[4]T. Ikari and Y. Koga, J. Phys. Soc. Jpn. Lett. **47**, 1017 (1979).
[5]J. L. Brebner, Can. J. Phys. **51**, 497 (1973).
[6]M. Cardona, *Modulation Spectroscopy*, Suppl. 11 of *Solid State Physics* (Academic, New York, 1969).
[7]J. Camassel, P. Merle, H. Mathieu, and A. Chevy, Phys. Rev. B **17**, 4718 (1978).
[8]G. Antonioli, D. Bianchi, and P. Franzosi, Appl. Opt. **18**, 3847 (1979).
[9]Y. Nishina and N. Kuroda, Physica **99B**, 357 (1980).